

ANALYTICAL SOLUTION OF HERMITE COLLOCATION DISCRETIZATION OF SELF-ADJOINT ORDINARY DIFFERENTIAL EQUATIONS

Stephen H. Brill
Department of Mathematics
Boise State University
Boise, Idaho, U.S.A.
email: `brill@math.boisestate.edu`

Abstract

We give herein analytical formulas for the solutions of a class of boundary value problems (BVPs) discretized by Hermite collocation. Specifically, our ordinary differential equations (ODEs) are self-adjoint, homogeneous, and have constant coefficients. Both Dirichlet and Neumann boundary conditions are considered. Analysis is provided which compares the discrete collocation solution to the continuous solution. Computational examples are given.

1 Introduction

The Hermite collocation discretization of differential equations has been much studied and a large literature has consequently resulted. However, to our knowledge, there are no results (prior to another paper by this author [1], in which the constant coefficient ODE $-D\frac{d^2u}{dx^2} + v\frac{du}{dx} = 0$ is studied) which provide analytical solutions to the systems of algebraic equations that arise from this discretization. This is in contrast to finite difference discretization which, for many linear differential equations, results in (block) tridiagonal matrix equations for which analytical formulas for the solution are available (see, for example, [2] and [3]).

This paper is organized as follows. We first describe Hermite collocation in the context of the ODEs under consideration. We then provide the analytical solution of matrix equations with the structure provided by the collocation discretization. A discussion of boundary conditions ensues. Subsequently, we provide an analysis which compares the discrete collocation solution to the continuous solution. We then study three example problems which illustrate the theory. A short section summarizing our results concludes the paper.

2 Hermite Collocation of Our ODEs

The differential equation we study is

$$\frac{d^2 u}{dx^2} + \rho u = 0, \quad (1)$$

defined on the interval $\mathcal{I} = [0, 1]$. Appropriate Dirichlet and/or Neumann boundary conditions are included. Here ρ is a real number. We partition the interval \mathcal{I} into m uniform subintervals, each of length h , by $0 = x_0, x_1, x_2, \dots, x_m = 1$. Note $x_j = jh$ and $mh = 1$.

The discretization proceeds by introducing a piecewise Hermite cubic interpolating polynomial

$$\hat{u}(x) = \sum_{j=0}^m [u_j f_j(x) + u'_j g_j(x)] \quad (2)$$

into the ODE (1), obtaining

$$\frac{d^2 \hat{u}}{dx^2} + \rho \hat{u} = E(x), \quad (3)$$

where $E(x)$ is an error function.

The Hermite basis functions, defined for $\eta \in [-\frac{1}{2}, \frac{1}{2}]$, are

$$f_j(x) = \begin{cases} f_L(\eta) = \frac{1}{2}(1+2\eta)^2(1-\eta), & x_{j-1} \leq x = x_j + \left(\eta - \frac{1}{2}\right)h \leq x_j \\ f_R(\eta) = \frac{1}{2}(1-2\eta)^2(1+\eta), & x_j \leq x = x_j + \left(\eta + \frac{1}{2}\right)h \leq x_{j+1} \\ 0, & \text{otherwise} \end{cases} \quad (4)$$

and

$$g_j(x) = \begin{cases} g_L(\eta) = \frac{h}{8}(2\eta+1)^2(2\eta-1), & x_{j-1} \leq x = x_j + \left(\eta - \frac{1}{2}\right)h \leq x_j \\ g_R(\eta) = \frac{h}{8}(2\eta-1)^2(2\eta+1), & x_j \leq x = x_j + \left(\eta + \frac{1}{2}\right)h \leq x_{j+1} \\ 0, & \text{otherwise.} \end{cases} \quad (5)$$

Note that \hat{u} in (2) interpolates the values $u_j = u(x_j)$ and $u'_j = \frac{du}{dx}(x_j)$, $j = 0, 1, \dots, m$, because $f_j(x_k) = \delta_{jk}$, $\frac{df_j}{dx}(x_k) = 0$, $g_j(x_k) = 0$, and $\frac{dg_j}{dx}(x_k) = \delta_{jk}$. Here δ_{jk} is the Kronecker symbol.

It is clear that (3) has $2(m+1)$ coefficients, namely u_j and u'_j , $j = 0, 1, 2, \dots, m$. However, the imposition of boundary conditions reduces this number to $2m$. To generate the $2m$ equations necessary to find these undetermined coefficients, we enforce that the error function $E(x)$ in (3) is identically zero at two distinct ‘‘collocation points’’ in the interior of each of the m subintervals.

Given certain smoothness conditions, the optimal (in terms of minimizing discretization error) location of the collocation points within each subinterval corresponds to the points of Gaussian quadrature [5]. In this work, we will use these optimal collocation points, which correspond to choosing the collocation points as

$j = 0, 1, \dots, m-1$. Here q_j and r_j represent, respectively, u_j and u'_j , $j = 0, 1, \dots, m$.

We begin by separately adding the two equations in (8) together and then subtracting the first from the second, obtaining the equations

$$A(q_j + q_{j+1}) + B(r_j - r_{j+1}) = 0 \quad (9)$$

$$C(q_j - q_{j+1}) + D(r_j + r_{j+1}) = 0, \quad (10)$$

$j = 0, 1, \dots, m-1$, where

$$A = c + a = \rho$$

$$C = c - a = \frac{1}{\sqrt{12}} \left(\frac{24}{h^2} - \frac{8}{3} \rho \right) \quad (11)$$

$$B = d - b = \frac{-2}{h} + \frac{\rho h}{6}$$

$$D = d + b = \frac{1}{\sqrt{12}} \left(\frac{12}{h} - \frac{\rho h}{3} \right).$$

We now state the main result of this paper.

Theorem 1 *Assume A , B , C , and D are all non-zero. Then the solution of (6), (8) and (9, 10) is*

$$q_j = \alpha_q \cos(j\theta - \chi) \quad (12)$$

$$r_j = \alpha_r \sin(j\theta - \chi), \quad (13)$$

$j = 0, 1, \dots, m$, where

$$\cos \theta = \frac{BC + AD}{BC - AD} \quad (14)$$

and the ratio

$$\frac{\alpha_q}{\alpha_r} = \frac{B}{A} \tan \frac{\theta}{2}. \quad (15)$$

Before proving this theorem, some comments are in order. First, one determines χ , α_q , and α_r by utilizing boundary conditions that are specified with (1). This is discussed in detail in Section 4. Secondly, and perhaps more interestingly, is the fact that $\cos \theta$ may have magnitude greater than unity, implying that θ is a imaginary number. This issue will be studied in Section 5. Finally, note that Theorem 1 holds in a setting more general than that of Hermite collocation. That is, Theorem 1 is true for *any* non-zero values of A , B , C , and D (which conform to the structure (9, 10)), not only those values given in (11). In particular, Theorem 1 holds for any value of $\xi \in (0, \frac{1}{2})$, not only for the value $\xi = \frac{1}{\sqrt{12}}$ (from which (7) and (11) were generated).

Proof We have

$$\begin{aligned} q_{j+1} &= \alpha_q \cos [(j\theta - \chi) + \theta] \\ &= q_j \cos \theta - \frac{\alpha_q}{\alpha_r} r_j \sin \theta \end{aligned} \quad (16)$$

Analogously, we have

$$r_{j+1} = r_j \cos \theta - \frac{\alpha_r}{\alpha_q} q_j \sin \theta. \quad (17)$$

Substituting (12), (13), (16), and (17) into the left sides of (9) and (10) gives

$$q_j \left[A(1 + \cos \theta) - B \frac{\alpha_r}{\alpha_q} \sin \theta \right] + r_j \left[B(1 - \cos \theta) - A \frac{\alpha_q}{\alpha_r} \sin \theta \right] \quad (18)$$

$$q_j \left[C(1 - \cos \theta) + D \frac{\alpha_r}{\alpha_q} \sin \theta \right] + r_j \left[D(1 + \cos \theta) + C \frac{\alpha_q}{\alpha_r} \sin \theta \right]. \quad (19)$$

We will be done when we show that the expressions in the four sets of brackets in (18) and (19) all vanish. Indeed, that (18) vanishes follows directly from (15). To show that (19) also vanishes, note that (14) implies that

$$\tan^2 \frac{\theta}{2} = -\frac{AD}{BC}. \quad (20)$$

Then utilize again (15). **Q.E.D.**

4 Boundary Conditions

We consider separately in each subsection below the four possible combinations of Dirichlet and Neumann boundary conditions. We shall show how the specification of boundary conditions allows us to determine the values of χ , α_q , and α_r . The boundary values b_0 , b_1 , b'_0 , and b'_1 are all real.

Case I: $u(0) = b_0$ and $u(1) = b_1$

Utilizing (12) for $j = 0$ and for $j = m$ and solving in each case for α_q gives

$$\alpha_q = \frac{b_0}{\cos \chi} \quad (21)$$

$$\alpha_q = \frac{b_1}{\cos(m\theta - \chi)}. \quad (22)$$

Eliminating α_q from (21) and (22) and solving for χ gives

$$\chi = \arctan \frac{\frac{b_1}{b_0} - \cos m\theta}{\sin m\theta}; \quad (23)$$

this choice provides that the two expressions for α_q found in (21) and (22) are equal. Now that we know α_q , we use (15) to find α_r .

Case II: $\frac{du}{dx}(0) = b'_0$ and $\frac{du}{dx}(1) = b'_1$

Utilizing (13) for $j = 0$ and for $j = m$ and solving in each case for α_r gives

$$\alpha_r = \frac{b'_0}{-\sin \chi} \quad (24)$$

$$\alpha_r = \frac{b'_1}{\sin(m\theta - \chi)}. \quad (25)$$

Eliminating α_r from (24) and (25) solving for χ gives

$$\chi = \arctan \frac{\sin m\theta}{-\frac{b'_1}{b'_0} + \cos m\theta}; \quad (26)$$

this choice provides that the two expressions for α_r found in (24) and (25) are equal. Now that we know α_r , we use (15) to find α_q .

Case III: $u(0) = b_0$ and $\frac{du}{dx}(1) = b'_1$

Use (12) for $j = 0$ and solve for α_q . Similarly, use (13) for $j = m$ and solve for α_r . We obtain

$$\alpha_q = \frac{b_0}{\cos \chi} \quad (27)$$

$$\alpha_r = \frac{b'_1}{\sin(m\theta - \chi)}; \quad (28)$$

and thus

$$\frac{\alpha_q}{\alpha_r} = \frac{b_0 \sin(m\theta - \chi)}{b'_1 \cos \chi}. \quad (29)$$

Use (15) and (29) and solve for χ :

$$\chi = \arctan \frac{-\frac{b'_1 B}{b_0 A} \tan \frac{\theta}{2} + \sin m\theta}{\cos m\theta}. \quad (30)$$

Then α_q and α_r are determined by using this value of χ in (27) and (28), respectively.

Case IV: $\frac{du}{dx}(0) = b'_0$ and $u(1) = b_1$

Use (13) for $j = 0$ and solve for α_r . Similarly, use (12) for $j = m$ and solve for α_q . We obtain

$$\alpha_q = \frac{b_1}{\cos(m\theta - \chi)} \quad (31)$$

$$\alpha_r = -\frac{b'_0}{\sin \chi}; \quad (32)$$

and thus

$$\frac{\alpha_q}{\alpha_r} = \frac{-b_1 \sin \chi}{b'_0 \cos(m\theta - \chi)}. \quad (33)$$

Use (15) and (33) and solve for χ :

$$\chi = \arctan \frac{-\cos m\theta}{\frac{b_1}{b'_0} \left(\frac{B}{A} \tan \frac{\theta}{2} \right)^{-1} + \sin m\theta}. \quad (34)$$

Then α_q and α_r are determined by using this value of χ in (31) and (32), respectively.

5 Comparison of Discrete and Continuous Solutions

In this section, we compare the discrete collocation solution of the ODE (1) with the continuous solution of the ODE (1). We initially separate our analysis depending upon the sign of ρ .

5.1 Comparison for $\rho > 0$

When $\rho > 0$, the solution of the ODE (1) is

$$u(x) = \beta \cos(\sqrt{\rho}x - \phi) \quad (35)$$

where β and ϕ are constants to be determined from the boundary conditions. We evaluate (35) and its derivative with respect to x at $x_j = jh$, obtaining

$$\begin{aligned} u(x_j) &= \beta \cos(j\sqrt{\omega} - \phi) \\ \frac{du}{dx}(x_j) &= -\sqrt{\rho} \beta \sin(j\sqrt{\omega} - \phi), \end{aligned} \quad (36)$$

where $\omega = \rho h^2$. Comparing (12) and (13) to (36), it is evident that it would be worthwhile to study the relationships between (14) and $\cos \sqrt{\omega}$ and between (15) and $-\rho^{-1/2}$. The former of these compares wavelength of the discrete and continuous solutions while the latter comparison between the discrete and continuous solutions focuses on the ratio of the amplitudes of the respective solution function and its derivative.

The wavelength of the continuous solution (35) is $2\pi\rho^{-1/2}$. Because of the piecewise cubic character of (2), collocation solutions can resolve wavelengths as small as h (see [4]) but not smaller. We thus want to ensure that ρ satisfies $2\pi\rho^{-1/2} \geq h$ or, equivalently,

$$0 < \omega \leq 4\pi^2. \quad (37)$$

A simple calculation using (11) shows that (14) becomes

$$\cos \theta = \frac{432 - 192\omega + 7\omega^2}{432 + 24\omega + \omega^2}. \quad (38)$$

We expand $\cos \sqrt{\omega}$ and (38) in Taylor series about $\omega = 0$:

$$\cos \sqrt{\omega} = 1 - \frac{1}{2}\omega + \frac{1}{24}\omega^2 - \frac{1}{720}\omega^3 + \mathcal{O}(\omega^4) \quad (39)$$

$$\frac{432 - 192\omega + 7\omega^2}{432 + 24\omega + \omega^2} = 1 - \frac{1}{2}\omega + \frac{1}{24}\omega^2 - \frac{1}{864}\omega^3 + \mathcal{O}(\omega^4). \quad (40)$$

A plot of these two curves is given in Figure 1. In examining Figure 1, we see that the two curves are visually indistinguishable from $\omega = 0$ to approximately $\omega = 9$. It is also worth noting (using (38)) that $\omega \in [0, 9]$ implies that $-1 \leq \cos \theta \leq 1$. That is, when we write $\cos \theta$ in this context, we are considering the real (i.e., not complex) valued version of the cosine. Thus we conclude, for these values of ω , that the collocation solution accurately represents the wavelength of the continuous solution. Note that these values of ω are well within the bounds (37) given above.

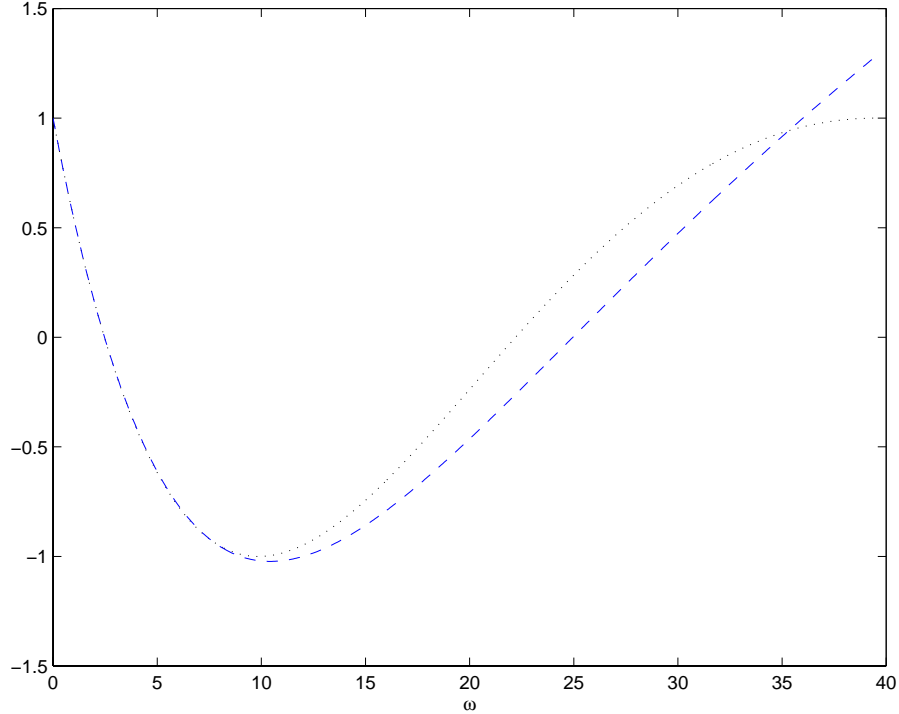


Figure 1: Dotted curve: $\cos \sqrt{\omega}$ (continuous), dashed curve: $\frac{432 - 192\omega + 7\omega^2}{432 + 24\omega + \omega^2}$ (discrete)

We now turn our attention to the comparison of the ratio of amplitudes for the continuous ($-\rho^{-1/2}$) and discrete (15) solutions. Utilizing (11) and (20), it is easily seen that this is equivalent to comparing ρ and $\rho R(\omega) = -\frac{AC}{BD}$, where

$$R(\omega) = \frac{-48(\omega - 9)}{(\omega - 12)(\omega - 36)}, \quad (41)$$

whose Taylor series expansion about $\omega = 0$ is

$$R(\omega) = 1 - \frac{1}{432}\omega^2 + \mathcal{O}(\omega^3)$$

and whose graph is depicted in Figure 2. We note that $R(\omega) \approx 1$ for $\omega \in [0, 2]$,

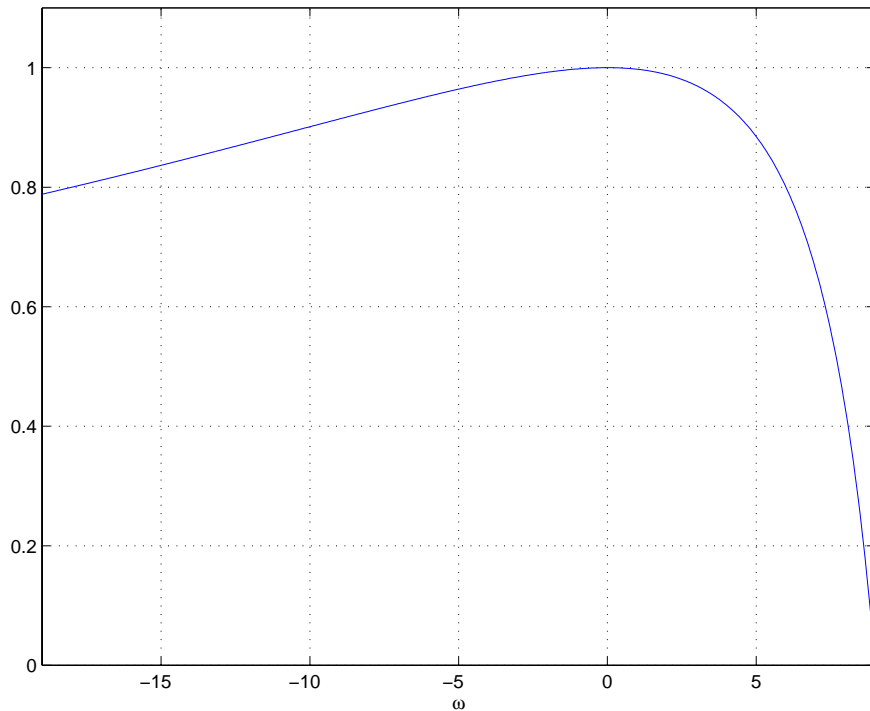


Figure 2: $R(\omega) = \frac{-48(\omega - 9)}{(\omega - 12)(\omega - 36)}$

beyond which $R(\omega)$ begins to move away from unity with increasing celerity. Thus, for $\omega \in [0, 2]$, there is excellent agreement concerning the amplitude ratio between the continuous and discrete solutions.

5.2 Comparison for $\rho < 0$

When $\rho < 0$, the solution of the ODE (1) is

$$u(x) = \gamma \cosh(\sqrt{-\rho}x - \psi) \tag{42}$$

where γ and ψ are real-valued constants to be determined from the boundary conditions. We evaluate (42) and its derivative with respect to x at $x_j = jh$, obtaining

$$\begin{aligned} u(x_j) &= \gamma \cosh(j\sqrt{-\omega} - \psi) \\ \frac{du}{dx}(x_j) &= \sqrt{-\rho}\gamma \sinh(j\sqrt{-\omega} - \psi). \end{aligned} \tag{43}$$

We now derive the discrete counterpart of (43). Note that $\rho < 0$ implies that $\omega < 0$, which in turn implies from (38) that $\cos \theta > 1$. Let $s = \cos \theta = \frac{432-192\omega+7\omega^2}{432+24\omega+\omega^2}$. Then, using the principal branch of the complex arccosine function, we obtain

$$\theta = -i \log p, \quad (44)$$

where $i = \sqrt{-1}$ and where

$$p = s + \sqrt{s^2 - 1}. \quad (45)$$

Note both $s > 1$ and $p > 0$ are real.

Because θ is imaginary, we see from (15) that the ratio $\frac{\alpha_q}{\alpha_r}$ is also imaginary. That is,

$$\frac{\alpha_q}{\alpha_r} = \frac{B}{A} \tan \frac{\theta}{2} = -\frac{B}{A} i \tanh \frac{\log p}{2} = -\frac{B}{A} i \frac{p^{1/2} - p^{-1/2}}{p^{1/2} + p^{-1/2}}. \quad (46)$$

Furthermore, we see that

$$\cos m\theta = \cosh(m \log p)$$

is real and

$$\sin m\theta = -i \sinh(m \log p)$$

is imaginary. Using the observations in this paragraph and (23), (26), (30), and (34), we conclude, irrespective of the value of the boundary conditions and of which type of boundary conditions are selected, that $\tan \chi$ is imaginary. Thus χ is also imaginary.

Therefore, (12) and (13) transform to

$$q_j = \alpha_q \cos(j\theta - \chi) = \alpha_q \cosh(j \log p - i\chi) \quad (47)$$

and

$$r_j = \alpha_r \sin(j\theta - \chi) = -i\alpha_r \sinh(j \log p - i\chi). \quad (48)$$

Note that the arguments of the hyperbolic functions in (47) and (48) are real. Thus q_j and r_j are real provided α_q is real and α_r is imaginary (which is consistent with the fact that the ratio $\frac{\alpha_q}{\alpha_r}$ is imaginary).

By analogy to the comparisons performed in Subsection 5.1, we now compare $\cosh \sqrt{-\omega}$ to $s = \frac{432-192\omega+7\omega^2}{432+24\omega+\omega^2}$. Because $\cosh \sqrt{-\omega} = \cos \sqrt{\omega}$, the Taylor series expansions are precisely those given in (39) and (40). The plot of the two curves under discussion appears in Figure 3. Note that Figure 3 is the continuation of Figure 1 into the left half-plane. We note that the two curves in Figure 3 are visually indistinguishable for $\omega \in [-6, 0]$. Thus we conclude, for these values of ω , that the collocation solution accurately represents the pseudo-wavelength of the continuous solution.

Again by analogy to Subsection 5.1, we now examine the ratio of the pseudo-amplitudes given by $(-\rho)^{-1/2}$ for the continuous case (see (43)) and $\frac{\alpha_q}{-i\alpha_r}$ (see (47) and (48)). As above, it is equivalent to compare ρ and $\rho R(\omega)$, where $R(\omega)$ is given in (41). The plot of $R(\omega)$ is found in Figure 2. We see that $R(\omega) \approx 1$ for $\omega \in [-2, 0]$. As ω decreases, $R(\omega)$ moves away from unity, although at a much slower rate when compared to how $R(\omega)$ moves away from unity as ω increases for $\omega > 2$. Thus we have excellent agreement vis-à-vis the ratio of the pseudo-amplitudes between the continuous and discrete solutions for $\omega \in [-2, 0]$.

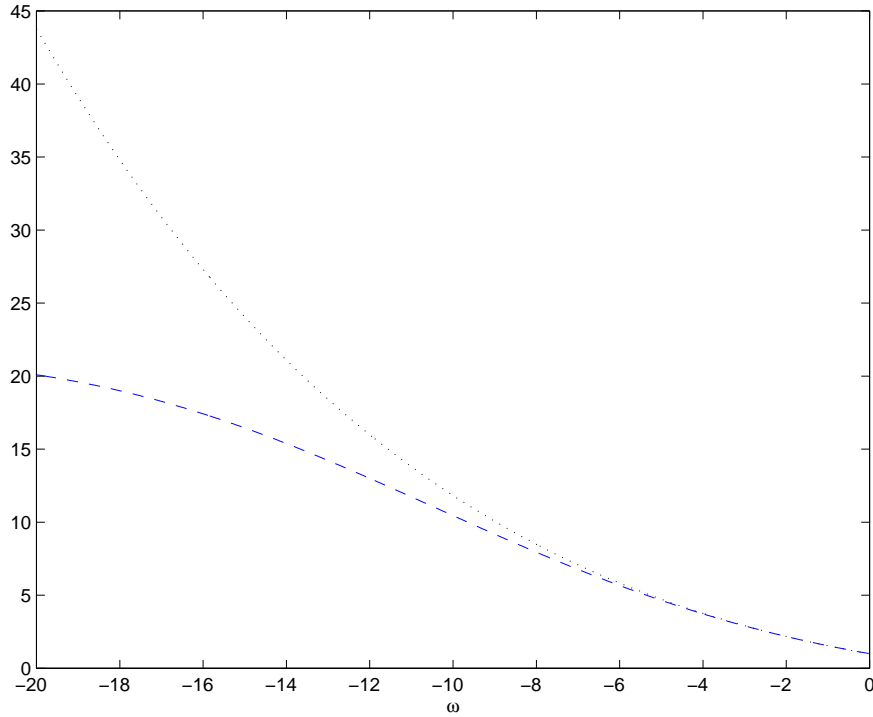


Figure 3: Dotted curve: $\cosh \sqrt{-\omega}$ (continuous), dashed curve: $\frac{432 - 192\omega + 7\omega^2}{432 + 24\omega + \omega^2}$ (discrete)

5.3 Comparison of phase shift parameters

Given the continuous solution the ODE (1) with $\rho > 0$ (i.e., (35)) with the Dirichlet boundary conditions $u(0) = b_0$ and $u(1) = b_1$, one may easily arrive at

$$\tan \phi = \frac{\frac{b_1}{b_0} - \cos \sqrt{\rho}}{\sin \sqrt{\rho}}. \quad (49)$$

The relationship between (23) and (49) is obvious, namely that $m\theta$ (for the discrete case) corresponds to $\sqrt{\rho}$ (for the continuous case). However, it is easy to see that this is equivalent to comparing $\cos \theta$ to $\cos \sqrt{\omega}$, which has already been discussed in detail in the contexts of wavelength and pseudo-wavelength. It is easy (but tedious) to show that the same correspondence holds regardless of the sign of ρ or what types of boundary conditions are selected. However, when we have one Dirichlet and one Neumann condition, the calculation of χ involves the ratio of amplitudes (or pseudo-amplitudes) which, according to our Taylor series analysis, is less accurate (by one order of magnitude) than the calculation of wavelengths (and pseudo-wavelengths). Therefore, the discussion pertaining to the wavelengths (and pseudo-wavelengths) of the continuous and discrete solutions holds also when considering the phase shift, with the caveat that one expects some decreased accuracy in the case when we have

one Dirichlet and one Neumann condition.

6 Examples

We discuss below three examples which illustrate the theory given above. The three examples correspond to $\rho = 0$, $\rho > 0$, and $\rho < 0$. Different types of boundary conditions will be considered.

6.1 Example: $\rho = 0$

When $\rho = 0$, (1) reduces to

$$\frac{d^2 u}{dx^2} = 0, \quad (50)$$

the graph of the solution of which is a non-vertical straight line, irrespective of boundary conditions (of course, Neumann boundary conditions at both $x = 0$ and $x = 1$ is disallowed in this example). In this case, $A = 0$ in (11) and therefore Theorem 1 does not apply. However, from (9) we obtain

$$r := r_0 = r_1 = \dots = r_m$$

and thus, from (10) and (11)

$$g_{j+1} = q_j + rh.$$

This is wholly consistent with the linear nature of the continuous solution of the differential equation. Additionally, since the interpolating polynomial (2) is piecewise cubic, the fact that the exact solution of the ODE (50) is obtained in this case from the collocation discretization is to be expected.

6.2 Example: $\rho > 0$

We consider the BVP

$$\begin{aligned} \frac{d^2 u}{dx^2} + 25u &= 0 \\ u(0) &= 1 \\ u(1) &= 2, \end{aligned} \quad (51)$$

whose continuous solution is

$$u(x) = \beta \cos(5x - \phi)$$

where

$$\phi = \arctan \frac{2 - \cos 5}{\sin 5} \approx -1.06130 \quad (52)$$

and

$$\beta = \sec \phi \approx 2.05027. \quad (53)$$

We will compute the collocation solution (12, 13) for $m = 20$. Thus $\omega = \frac{1}{16}$ and so, from (38),

$$\theta \approx 0.250000.$$

Therefore, from (11) and (15), we have

$$\frac{\alpha_q}{\alpha_r} \approx -0.200001.$$

Also, from (23),

$$\chi \approx -1.06130$$

(compare with (52)). Now, both (21) and (22) give

$$\alpha_q \approx 2.05027$$

(compare with (53)) and so, using (15),

$$\alpha_r \approx -10.2513.$$

So the collocation solution of (51) is

$$\begin{aligned} u_j = q_j &\approx 2.05027 \cos(0.250000j + 1.06130) \\ u'_j = r_j &\approx -10.2513 \cos(0.250000j + 1.06130). \end{aligned}$$

6.3 Example: $\rho < 0$

We consider the BVP

$$\begin{aligned} \frac{d^2 u}{dx^2} - 16u &= 0 \\ \frac{du}{dx}(0) &= 0 \\ u(1) &= -3, \end{aligned} \tag{54}$$

whose continuous solution is

$$u(x) = \gamma \cosh(4x - \psi)$$

where

$$\psi = 0 \tag{55}$$

and

$$\gamma = \frac{-3}{\cosh 4} \approx -0.109857. \tag{56}$$

We will compute the collocation solution for $m = 20$. Thus $\omega = -\frac{1}{25}$ and so, from (45),

$$p \approx 1.22140;$$

thus, from (44),

$$\theta \approx -0.200000 i.$$

Now, consider (32). Since $b'_0 = 0$ in (32), the only way that (32) can avoid being undefined (but merely indeterminate) is to require that

$$\sin \chi = 0.$$

Because $\rho < 0$, we know that χ is imaginary. Thus

$$\chi = 0i = 0$$

(compare with (55)). Thus

$$\alpha_q = \frac{-3}{\cos m\theta} \approx -0.109857$$

(compare with (56)). Therefore, using (15), we have

$$\alpha_r \approx -0.439428 i.$$

Thus, from (47) and (48), the collocation solution of (54) is

$$\begin{aligned} u_j = q_j &\approx -0.109857 \cosh(0.200000j) \\ u'_j = r_j &\approx -0.439428 \sinh(0.200000j). \end{aligned}$$

7 Summary and conclusions

In this paper, we provide analytical solutions to matrix equations that have the structure corresponding to the Hermite collocation discretization of self-adjoint, one-dimensional, constant coefficient ordinary differential equations defined on a uniform mesh. Results are given which hold for any combination of Dirichlet and Neumann boundary conditions. Taylor series analysis indicates very good agreement between the continuous solution of the BVP and the discrete collocation solution for a wide range of parameter values. The algorithm for determining the analytical form of the collocation solutions is not complicated and is easily implemented.

References

- [1] S. H. Brill, *Analytical Solution of Hermite Collocation Discretization of the Steady-State Convection-Diffusion Equation*, International Journal of Differential Equations and Applications, **4** (2002), 141–155.
- [2] P. DuChateau and D. W. Zachmann, *Partial Differential Equations*, McGraw-Hill, New York, 1986.
- [3] K. W. Morton, *Numerical Solution of Convection-Diffusion Problems*, Chapman & Hall, London, 1996.
- [4] G. F. Pinder and A. Shapiro, *A New Collocation Method for the Solution of the Convection-Dominated Transport Equation*, Water Resources Research, **15** (1979), 1177–1182.
- [5] P. M. Prenter, *Splines and Variational Methods*, John Wiley & Sons, New York, 1975.